



DEUTSCHES ELEKTRONEN-SYNCHROTRON **DESY**

POSSIBLE OPEN CHANNEL EFFECTS IN THE CHARMONIUM SPECTRUM

by

I.M. Barbour

Glasgow University

J.P. Gilchrist

Deutsches Elektronen-Synchrotron DESY, Hamburg

ISSN 0418-9833

NOTKESTRASSE 85 · 2 HAMBURG 52

DESY behält sich alle Rechte für den Fall der Schutzrechtserteilung und für die wirtschaftliche Verwertung der in diesem Bericht enthaltenen Informationen vor.

DESY reserves all rights for commercial use of information included in this report, especially in case of filing application for or grant of patents.

To be sure that your preprints are promptly included in the
HIGH ENERGY PHYSICS INDEX,
send them to the following address (if possible by air mail) :

DESY
Bibliothek
Notkestrasse 85
2 Hamburg 52
Germany

Possible open channel effects in the charmonium spectrum

by

I.M. Barbour

Glasgow University

J.P. Gilchrist

Deutsches Elektronen-Synchrotron DESY, Hamburg

Abstract

The non-relativistic quark model is used to investigate the effects of open channels and possible $(q\bar{q})^2$ dimesonium states on the charmonium spectrum. An alternative interpretation of the structures in R above threshold is proposed.

Considerable attention has been given in the past to non-relativistic quark model interpretations of the structure in R (1,-,5) in the charmonium region. With the exception of Ref. (5), which interpretes the structure at 4.028 GeV as a $D^* \bar{D}^*$ molecule, most authors explained the branching ratios into $D\bar{D}$, $D^* \bar{D}$ and $D^* \bar{D}^*$ there via a 3S charmonium state at 4.028 GeV and a 2D state at 4.16 GeV; the smallness of the observed decay ratios then arises through the nodes in the 3S wavefunction.

Problems arise, however, in that it is difficult to obtain sufficient mixing of the 2D and 3S states to give the clear double peak structure (Fig. 8). Bradley & Robson (3) considered higher order Q.C.D. corrections to $e^+e^- \rightarrow c\bar{c}$ which couple the 2D states directly to e^+e^- and hence enhance the 4.16 GeV peak. They empirically reproduce R using experimental couplings without introducing open channels. However, it is difficult to explain the large widths for the D-wave states to e^+e^- which are required for this interpretation of R.

Eichten et al. (4) used a coupled channel model with predominantly long range vector interaction to interpret these structures in R as arising from the 3S and 2D states at 4.028 and 4.16 GeV, respectively. In this paper we use their model with the standard short range vector and long range scalar interaction. This picture predicts the observed bound state spectrum but leads to the decay matrix elements being controlled predominantly by strong cancellations between the short, medium and long range components of the quark pair creation 'potential'. As an alternative interpretation of the data we identify the structure in R at 3.68 GeV and 4.16 GeV as the 2S and 3S radial excitations. Interference between these states then produces the structure in R at approx. 4.03 GeV, just above the $D^* \bar{D}^*$ threshold.

The Model

The interaction Hamiltonian we use contains a medium to long range part as a Lorentz scalar:

$$H_S = \frac{1}{2} \sum_f \int d^3r d^3r' \bar{\Psi}_f(r') \Psi_f(r) \left\{ a |r'-r| + 2b_s \right\} \bar{\Psi}_f(r) \Psi_f(r) \quad (1)$$

and for the short to medium range vector interaction:

$$H_V = \frac{1}{2} \sum_f \int d^3r d^3r' \bar{\Psi}_f(r') \frac{\lambda_a}{2} \Psi_f(r) \left\{ \frac{\alpha_s}{|r'-r|} + 2b_v \right\} \bar{\Psi}_f(r) \frac{\lambda_a}{2} \Psi_f(r) \quad (2)$$

where f runs over quark flavours. The 'string constant' a is taken to be 0.23 GeV^2 and to be proportional to the square root of the Casimir for the representation of the objects at the ends of the string (here only 8-8 at high mass). The Q.C.D. coupling α_s is taken to be 0.31 GeV , b_s and b_v are possible constant contributions to the medium range part of the potential. This interaction has been used in fits to the charmonium (1,3,4,6) and baryon spectra (7).

Lowest order calculation of the masses, relativistic corrections and mixings from this potential involves interactions of the diagrammatic form:



Fig. 1

These lead to the usual non-relativistic quark model potential

$$V(r'-r) = a |r'-r| - \frac{4}{3} \frac{\alpha_s}{|r'-r|} + 2b \quad (3)$$

where

$$b = b_v + b_s$$

Calculation of quark pair production through diagrams of the form:

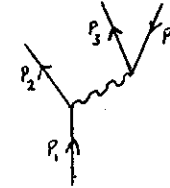


Fig. 2

is independent of b_v . The long range part of the potential and b_s contribute strongly to the decay amplitude through this interaction. As we shall see, a fit to the decay widths and spectrum requires that there is a large cancellation between these two terms in the amplitude for decays and that consequently the medium range interaction is predominantly scalar ($b_s \gg b_v$).

The calculation is performed using the coupled channel model of Eichten et al.

(4). We include $c\bar{c}$ states and $c\bar{c}q\bar{q}$ states with $q = u, d, s$ and $m_u = m_d = 0.335 \text{ GeV}$, $m_s = 0.45 \text{ GeV}$ and $m_c = 1.84 \text{ GeV}$. Possible mixings of two and four quark states through a u - d mass difference should only contribute very near to thresholds and not affect our general conclusions.

The set of four quark meson-meson states considered contains only the spin excited F and D states of the form $D\bar{D}$, $D^*\bar{D} + D\bar{D}^*$ and $D^{*-}\bar{D}^+$. The next highest state will contain the P wave excitation of one D meson with a threshold of 4.4 GeV . Consequently we consider only the ground state and first radial excitations for the $1 = 0, 1, 2$ $c\bar{c}$ system together with the $3S$ excitations and fit to the region below 4.3 GeV .

As well as colour singlet-singlet configurations for the four quark system one can have $(c\bar{q})^8 - (\bar{c}q)^8$ dimensionium bound states. We have included the effects of these states in the approximation that the angular momentum is between the octet mesons. This is akin to the $D\bar{D}$ meson configurations, the omission of the other

angular momentum configurations will affect mixings between the states but should only be important at higher energies.

The $c\bar{c}$ charmonium states couple to $(c\bar{q})^4 - (\bar{c}q)^4$ and $(c\bar{q})^8 - (\bar{c}q)^8$ via the pair creation terms in the potential (Fig. 2). The dimensioniums can also couple to the meson-meson states via the one gluon exchange term by rearranging the colour within the molecule.

Thus the physical charmonium states can be written as

$$|C_{J_1}^T(p_n); \lambda\rangle = \sum_n a_n^\lambda |(c\bar{c})_{J_1}^T(p_n); n\rangle + \sum_m b_m^\lambda |(c\bar{q})^4 - (\bar{c}q)^4(p_n); m\rangle + \sum_l \sum_p \alpha_l^\lambda(p, p_n) |(M_1 \bar{M}_2)_{S_2}^S(p); l\rangle \quad (4)$$

i.e. as a superposition of $c\bar{c}$ states with total spin 1, octet-octet dimesonium, and meson-meson states ($1 = D\bar{D}, D\bar{D}^* + \bar{D}D^*, D^*\bar{D}^*$ etc.) with relative momentum p .

For the singlet two quark states:

$$|(c\bar{c})_{J_1}^T(p_n); n\rangle = \sum_{i,j} \sum_{p_1, p_2} \delta(p_n; p_1 + p_2) \psi_{c, \bar{c}}^{ij}(p_1, p_2) \cdot \frac{\delta_{ij}}{\sqrt{3}} c_{c, c}^{i\dagger}(p) d_{\bar{c}, \bar{c}}^{j\dagger}(p_2) |0\rangle \quad (5)$$

where c^\dagger and \bar{c}^\dagger create quark c and antiquark \bar{c} , respectively. The spacial wave functions are taken in a Gaussian basis:

$$\phi(r_1, r_2) = \sum_i c_i e^{-\alpha_i(r_1 - r_2)^2} |r_1 - r_2|^L Y_L^M(\hat{r}_1 - \hat{r}_2) \quad (6)$$

where c_i, α_i are obtained by a variational solution to the two-body Schrödinger

equation. The meson-meson states are given by:

$$|(M_1 \bar{M}_2)_{S_2}^S(p); l\rangle = \sum_{S_1 \bar{S}_1} C_{S_1 \bar{S}_1}(S_1 S_2; S_2 \bar{S}_2) |(c\bar{q})_{S_1}^S(p), (\bar{c}q)_{\bar{S}_1}^S(-p)\rangle \quad (7)$$

neglecting any final state interactions between the mesons.

The other four quark states are given by a generalization of equations (5) and (6). They are obtained following the method described by Barbour and Ponting (8) extended to the unequal mass case. As will be seen, they play no significant role in the fit to the data but do indicate in part the influence of the higher energy four quark states on the mass-spectrum generated below.

The masses of all these states and their wavefunctions were obtained by a stochastic variational technique (9). The spectrum (no mixing) and scales for both the charmonium and the D and F mesons are summarized in tables (1) and (2). Since the variational procedure loses accuracy for the higher radial excitations, we obtained the 3S $c\bar{c}$ wavefunction by orthogonality to the 1S and 2S states together with the minimisation of the mass and the requirement (10):

$$\Gamma_{3S \rightarrow e^+ e^-} = 0.7 \text{ keV} = \frac{16 \pi e_Q^2 \alpha^2}{m_Q^2} |\Phi(0)|^2 \quad (8)$$

$$\text{or } \psi(0) = 0.1 \text{ GeV}$$

In order to calculate the mixing between these states and the masses of the physical $c\bar{c}$ states we follow Eichten et al. (4) and study the bound state sector resonant:

$$G(z) = (H_0 - z + \Omega(z))^{-1} \quad (9)$$

The renormalized masses are determined from the location of the poles in the resolvent. Matrix elements of $\Omega(z)$, between the charmonium and di-mesonium bound states $|\mathcal{B}_{J_1}^T(P_m); m\rangle$ can be expressed as

$$\Omega_{mn}(E) = \sum_{\ell, s_1, s_2} V \int \frac{d\Omega_p}{(2\pi)^3} \left\{ \int_{m_p}^{\infty} d\xi |p| \frac{E_1 E_2}{\xi} \left[\frac{1}{E - \xi} - i\pi \delta(E - \xi) \right] \right. \\ \left. \langle \mathcal{B}_{J_2}^T; n | H_T | (M_1 \bar{M}_2)_{s_1}^S(p); \ell \rangle \langle (M_1 \bar{M}_2)_{s_2}^S(p); \ell | H_T | \mathcal{B}_{J_1}^T; m \rangle \right\} \quad (10)$$

where m_p is the threshold energy for a given meson-meson decay sector state characterized by l . If the D^* and D masses are degenerate then it follows that (4)

$$\sum_{\ell=1}^3 \langle S \text{ wave} | H_T | (M_1 \bar{M}_2)_{s_1}^S(p); \ell \rangle \langle (M_1 \bar{M}_2)_{s_2}^S(p); \ell | H_T | D \text{ wave} \rangle = 0 \quad (11)$$

and all mixing between S and D states through open channels vanishes (also for F mesons). Though there is still mixing due to the tensor force.

However, if we separate the thresholds so that despite the equal mass approximation the $D\bar{D}$ channel opens at 3.72 GeV, the $D^*\bar{D}$ at 3.86 GeV and the $D^*\bar{D}^*$ at 4.012 GeV, there will be a contribution to the imaginary term in (10) from the pole, if one of the states lies between 3.72 GeV and 4.012 GeV. For both states outside or inside this region mixing again vanishes.

Phase space factors will break this rule via mass difference (see eqn. 11). However, it is because of this effect that it is difficult to obtain large mixing of the 2D and 2S (as suggested by the experimental data) since their masses are greater than the $D^*\bar{D}^*$ threshold, whereas reasonable mixing can be

obtained for the 1D to 2S since the mass of the 1D state lies between the $D\bar{D}$ and $D^*\bar{D}$ thresholds thus giving it a contribution to R.

There is no such selection rule for mixing within the S waves or D waves alone, and we shall see that there mixing can be large. As all our wavefunctions are Gaussian, analytic expressions can be obtained for the overlap integrals of the state with the Hamiltonian.

The Hamiltonian interaction of equation (1) for a diagram of the form of Fig. 1 is

$$\frac{1}{2} \int d^3r d^3r' \frac{1}{2m_3} \xi_{s_3}^+ \sigma \xi_{s_4} (p_3 - p_4) \delta_{s_1 s_2} (a|r-r'| + 2b) e^{i[(p_3+p_4) \cdot r - (p_1+p_2) \cdot r']} \quad (12)$$

in the non-relativistic limit, notice that the pair is created in a 0^{++} . Similarly if the vector form is taken we obtain:

$$\frac{1}{2} \int d^3r d^3r' \frac{1}{2m_3} \xi_{s_3}^+ \sigma \xi_{s_4} (p_3 + p_4) \delta_{s_1 s_2} \left\{ \frac{\kappa_1}{|k - r'|} + 2b_v \right\} e^{i[(p_3+p_4) \cdot r - (p_1+p_2) \cdot r']} \quad (13)$$

where here the pair is created in a state 1^{--} and that the constant vector part b_v does not contribute.

The amplitude for the decay of a pure $c\bar{c}$ bound state (angular momentum L) to two mesons (angular momentum l) is

$$\langle (M_1 \bar{M}_2)_{s_2}^S(p_m); n | H_T | (c\bar{c})_{J_1}^T; \lambda \rangle = \sum_{\ell, m} \mathcal{L}_{\ell}^L(p_m) \cdot C_{\ell s} (T J_2; m s_2) Y_{\ell}^m(\hat{p}_2) \\ \sqrt{(2S+1)(2\ell+1)} \begin{Bmatrix} L_{cc} & S_{cc} & 1 \\ s & \ell & 1 \end{Bmatrix} \\ \sqrt{3(2S_m+1)(2S_{\bar{m}}+1)(2S_{cc}+1)} \begin{Bmatrix} \frac{1}{2} & \frac{1}{2} & S_m \\ \frac{1}{2} & \frac{1}{2} & S_{\bar{m}} \\ S_{cc} & 1 & S \end{Bmatrix} \quad (14)$$

where $\mathcal{L}(P_n)$ contains the spatial structure of the interaction. We assume di-mesonium states decay to two mesons predominantly via one gluon exchange, the amplitude for this has a similar structure to that of equation (14). Similar expressions can be obtained for the overlap of the $c\bar{c}$ state with the di-mesonium.

Results

We first comment on the effects of the bound dimesonium states on the mass spectrum of the charmonium system. Not unexpectedly, because of their high mass, their effects as shown in table (3) are small, leading to mass shifts of approx. -40 MeV in the S-wave states. Only p-wave dimesonium are included. Note that the general trend is to shift the 1^{--} states down in mass.

When we include the open channel contributions with the potential parameters for table (1) we will find it necessary to shift some of the states downwards in order to obtain a fit to the structure in R. (Note: because of the strong cancellation between the contributions from the linear component of the potential and b_s it is possible to adjust the potential parameters and fit the low energy (< 4 GeV) mass spectrum when the open channel contributions are included without arbitrary mass shifts. However, we could not simultaneously obtain with this potential the double peak structure in R above 4 GeV with or without ad hoc mass shifts.) It is not inconsistent to attribute these shifts to additional dimesonium states and the effects of open channels omitted ($D\bar{D}_p$ etc.)

The structure of the decay amplitudes is shown in Fig. 3. The contributions from the long range and medium range parts of the interaction are nearly equal

in magnitude but opposite in sign, hence the difficulty in interpreting the structures in R within this model. When $2b_s = -0.7$ GeV most of the amplitudes are similar to those calculated in the vector model of Eichten aside from the 1^3D_1 , (and p-waves) in which the cancellation with the one gluon exchange amplitude is almost total at the decay momentum.

The mixings between the two and four quark states depend predominantly on the nearby singlet-singlet open channel contributions which as described above depend strongly on the cancellation between the scalar amplitudes. The charmonium states contribute to R via

$$\Delta R(E) = \frac{6\pi}{E^2} \cdot 16 \sum_{n,m} \text{Im} g_{nm} \{ \phi_n^*(0) \mathcal{L}_{nm}(E) \phi_m(0) \} \quad (15)$$

where the $\phi_n(0)$ are the $c\bar{c}$ wave functions at the origin and $\mathcal{L}_{nm}(E)$ contains the mixings of the various states. Thus D wave $c\bar{c}$ and 4 quark dimesonium states obtain structure in R only through mixing with the S wave $c\bar{c}$ states.

Fig. 4 shows the structure in R obtained for $2b_s = -0.75$ GeV which gives weak coupling for $3D_1$ to $D\bar{D}$. Here the 3S state has been shifted to 4.07 GeV and the 2D left at 4.265 GeV. If we try to reproduce the double peak in R by lowering the 2D mass a single peak structure is still obtained. This is a consequence of equation (11) since the 3S and 2D are both above the $D^* \bar{D}^*$ threshold and the strange quark contribution to R is small. On the other hand the 2S and 1D states stand on either side of a threshold and so mix, the mixing being controlled by the degree of cancellation.

We therefore find that if the 2D and 3S states are above the $D^* \bar{D}^*$ threshold then the 2D state cannot mix strongly and contribute to R. For $2b_s = -0.75$ GeV no clear double peak structure could be obtained. The 2D state could couple

directly through higher order QCD corrections

$$\Gamma_{e^+e^-} = \frac{200 \frac{4}{9} \alpha^2}{M^6} |\psi''(0)|^2 \quad (16)$$

For the 1D and 2D wavefunctions used this gives

$$\Gamma_{1D \rightarrow e^+e^-} = 0.03 \text{ keV} \quad \Gamma_{2D \rightarrow e^+e^-} = 0.07 \text{ keV} \quad (17)$$

both small compared with the data.

We now consider $2b_s = -0.7$ GeV and vary the mass of the 3S between 4.03 GeV and 4.235 GeV. At 4.03 GeV a single peak structure is obtained and as above the 2D is essentially decoupled. At 4.235 GeV a double peak structure was obtained Fig. 5. The peak at 4.05 GeV is not associated with the 2D but rather with the opening of the $D^* \bar{D}^*$ threshold interfering with the nearby 3S state. At 4.19 GeV a single peak structure reappears just above the $D^* \bar{D}^*$ threshold Fig. 6. Table (3) shows the new (renormalized) masses.

From the above we conclude that if R exhibits a double peak structure between 4.0 GeV and 4.2 GeV it is not possible in this model to assign the 2D as a contributing state. The model requires that the structures be associated with the 3S and the nearby threshold. However, ΔR as predicted by the model is of the order 0.25 that of the data. That we associate with underestimating the 3S wavefunction at the origin. If we had included the QCD factor $(1-16/3 \cdot \frac{\alpha_s}{\pi}) \approx 1/2$ in the Van-Royen-Weisskopf formula the 3S would be increased by a factor of $\sqrt{2}$ at the origin. To allow for the further effects of mixing reducing the contribution of the 3S to R we shall rather take double the wavefunction at the origin. Fig. 7 shows ΔR calculated for this modified 3S wavefunction at 4.19 GeV and $2b_s = -0.7$ GeV (a single enhanced peak is obtained for $2b_s = -0.75$ GeV).

The mechanism giving rise to this structure is shown in Fig. 8, where we plot the dominant contributions to $\text{Im}(\mathcal{G}_{\text{ann}}(E))$. In the $D^* \bar{D}^*$ contribution the 3S-2S interference term is constructive below 4.1 GeV and destructive above and when combined with $D^* \bar{D}$ contributions the lower peak is enhanced. Unfortunately in the $2b_s = -0.7$ GeV case the lower energy structure (the 2S peak at 3.78 GeV) has been smeared out due to the appearance of an extra node in the decay amplitude through the cancellation effect. We do not believe that this affects the interference effects between the 2S and 3S which depends on the higher momentum part of the amplitude. Also the interference effect is present in the $2b_s = -0.75$ GeV case but to a lesser degree.

Finally we plot our structure in R above 3.85 GeV on the non-charmed contribution including the tau lepton and compare with the DASP data (11), Fig. 9. This data is also in agreement with the CRYSTAL BALL results (12). The open channel contributions at the 'phase space' peak are in the ratios

$$R_{D^* \bar{D}} : R_{D^* \bar{D}^*} : R_{D \bar{D}} = 1 : 0.49 : 0.014 \quad (18)$$

and at the 3S peak 1:0.13:0.02.

We mention here that it was not necessary for the ratios equation (18) to have a zero in the 3S decay amplitude $D \bar{D}$ channel near 4.03 GeV as suggested by some authors (3,4,10). However, in our ratios at the 3S peak the node in the $D \bar{D}$ channel is nearby and consequently that ratio to $D^* \bar{D}^*$ is sensitive to changes in its position.

Given that the interference effects and nearby thresholds can produce peaks in the data it would be dangerous to interpret any structures in this region

as gluoniums. The non-relativistic quark model cannot give a unique interpretation of the data above 3.8 GeV, but suggests weak coupling of the 2D to e^+e^- and only the 3S state in the 4.15 GeV region. We also noted that the effects of 4q (dimesonium) states in this region was negligible.

Acknowledgements

We would like to thank D.K. Ponting and A. Nishimura for useful discussions. I.M.B. would like to thank Tom Walsh for the hospitality of the DESY Theory Group during part of this work and J.P.G. would like to acknowledge the financial assistance of the Royal Society and the S.E.R.C.

References

- 1) T. Appelquist et al., Phys. Rev. Lett. 34 (1975) 365;
B.J. Harrington et al., Phys. Rev. Lett. 34 (1975) 706
- 2) J.L. Richardson, Phys. Rev. Lett. 82B (1979) 272;
J. Kogut and L. Susskind, Phys. Rev. Lett. 34 (1975) 767
- 3) A. Bradley and D. Robson, Manchester preprint (1979) to appear in Z. Physik C
- 4) Eichten et al., Phys. Rev. D 17 (1978) 3090 and D 21 (1980) 203
- 5) L.B. Okun and M.B. Voloshin, Zh. Eksp. Theor. Fiz 23 (1976) 369;
A. De Rujula, H. Georgi, S.L. Glashow, Phys. Rev. Lett 38 (1976) 317;
M. Bander, G.L. Shaw, P. Thomas, S. Meshkov, Phys. Lett. 36 (1976) 695;
C. Rosenzweig, Phys. Rev. Lett. 36 (1976) 697;
A. De Rujula and R.L. Joffe, Proc. Conf. Exptl. Meson Spectroscopy,
Northeastern Univ. Boston (April 1977);
F. Gutbrod, G. Kramer and Ch. Rumpf, Z. Physik C (1979) 391
- 6) R. Barbieri, B. Koyerler, R. Gatto, Z. Kunszt, Nucl. Phys. B105 (1976) 215
- 7) I.M. Barbour and D.K. Ponting, Z. Physik C (1980) 119
- 8) I.M. Barbour and D.K. Ponting, Z. Physik C (1980) 221
- 9) V.I. Kukulín and V.M. Krasnopolsky, J. Phys. G 3(1977) 795
- 10) G. Wolf, DESY preprint 80/13
- 11) R. Brandelik et al., Phys. Lett. 76B (1978) 361
- 12) K.H. Mess and B.H. Wiik, DESY preprint 82/11

Table 1

The masses of the "naive" states, scales and coefficients for the wave-functions of equation (6) with $\alpha_s = 0.31$, $a = 0.23 \text{ GeV}^2$, $2b_s = -0.7 \text{ GeV}$.

State	Mass (GeV)	Scales $\alpha_i (\text{GeV}^2)$				Coefficients C_i			
		α_1	α_2	α_3	α_4	c_1	c_2	c_3	c_4
1^3S_1	3.155	0.215	0.093	0.999	-	0.819	0.108	0.442	-
2^3S_1	3.788	"	"	"	-	0.794	-0.497	0.210	-
$\bar{c}c$ 3^3S_1	4.430	"	"	"	0.243	-10.894	0.666	-0.50	10.857
1^3D_1	3.894	0.321	0.074	0.145	-	0.187	0.103	0.870	-
2^3D_1	4.33	"	"	"	-	0.210	-0.151	0.410	-
Dimesonium p wave state	Mass (GeV)	Scales *							
		$\xi (\text{GeV}^2)$	$\chi (\text{GeV}^2)$						
$\bar{c}c(\frac{u\bar{u}+d\bar{d}}{\sqrt{2}})$	6.121	0.117	0.089						
$\bar{c}c s s$	6.163	0.108	0.088						

* The dimesonium states have an H configuration, the scale χ relates to the cross-strut binding the quark-antiquark pairs and the ξ to the binding between the quark antiquark at each end. Only one basis state is taken in the expansion with coefficient unity. The wave-function is otherwise similar to that of equation (6).

Table 2

D and F meson masses and scales with only one gaussian basis state, and the potential parameters α_s and $2b$ for the fit to the experimental masses ($a = 0.23 \text{ GeV}^2$).

state	mass (GeV)	scales, $\chi (\text{GeV}^2)$	α_s	$2b (\text{GeV})$
D	1.863	0.91	0.56	- 0.93
D*	2.006			
F	2.030	0.106	0.46	- 0.86
F*	2.140			

Table 3

Masses of states after mixing within bound state sector and also for inclusion of open channels ($2b = -0.7 \text{ GeV}$)

State	Mass (GeV)	
	Bound state mixing only	'Full renormalized' mass
1^3S_1	3.115	3.065
2^3S_1	3.742	3.70
3^3S_1	4.428	4.19 *
1^3D_1	3.891	3.78 **
2^3D_1	4.330	4.285

* 0.25 GeV has been subtracted by hand

** 0.065 GeV has been subtracted by hand

Figure Captions

Fig. 3 The decay amplitudes for the 3S_1 charmonium state into two mesons as defined by equation (14). The relative momentum of the mesons is p . The high cancellation between the linear and constant contributions is typical.

Fig. 4 The charm contribution to R from exclusive channels as defined by equation (15), in the region $3.7 < E < 4.2$ GeV. The fit here is with $2b_s = -0.75$ GeV. Only the largest contributions in R are indicated in the figure.

Fig. 5 The charm contribution to R from exclusive channels in the region $3.8 < E < 4.3$ GeV. The fit here is with $2b_s = -0.7$ GeV.

Fig. 6 Same as fig. 5 but with the 3S_1 state shifted lower in mass.

Fig. 7 ΔR calculates with the same parameters as used in fig. 6 but with the wavefunction of the 3S_1 , at the origin constrained to be twice as large.

Fig. 8 The various contributions to ΔR from equation (15) that give figure 7 when summed.

Fig. 9 The theoretical structure in R taken from figure 7 with the non-charmed and tau lepton contributions added, also shown, the experimental data from the DASP collaboration (11).

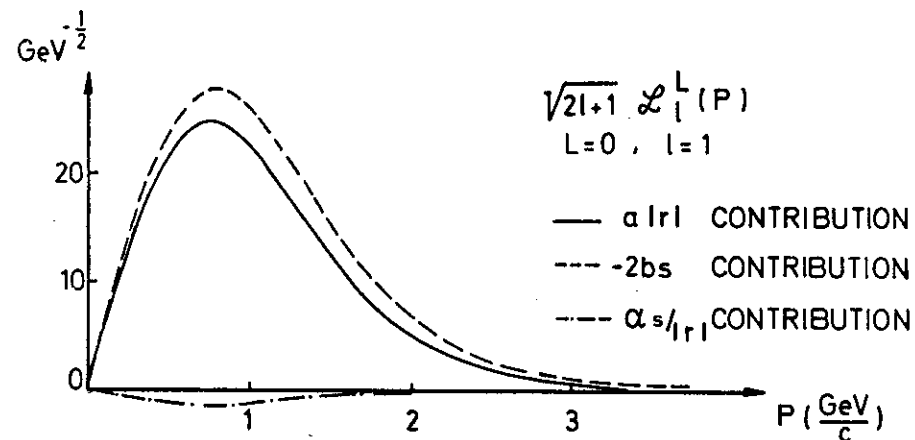


Fig.3

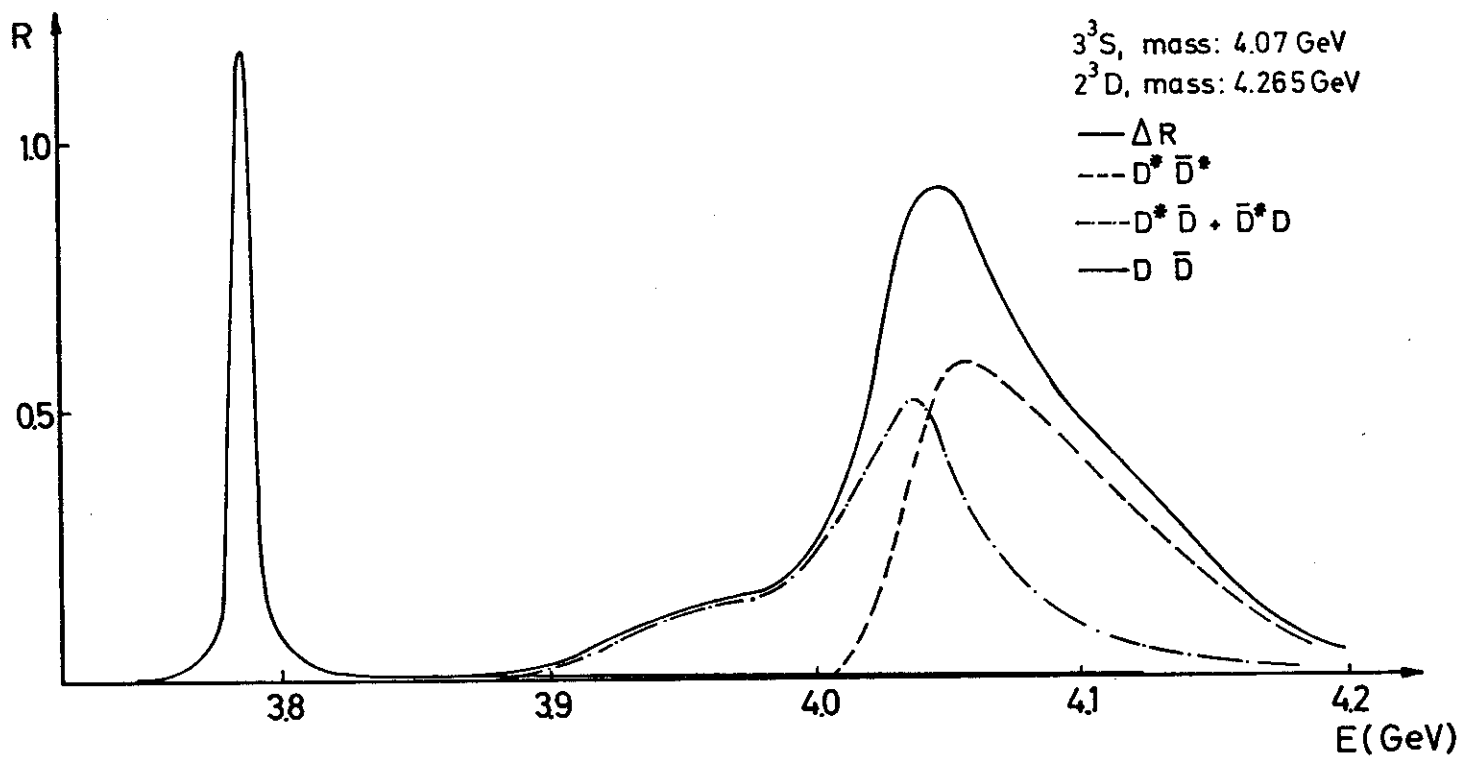


Fig.4

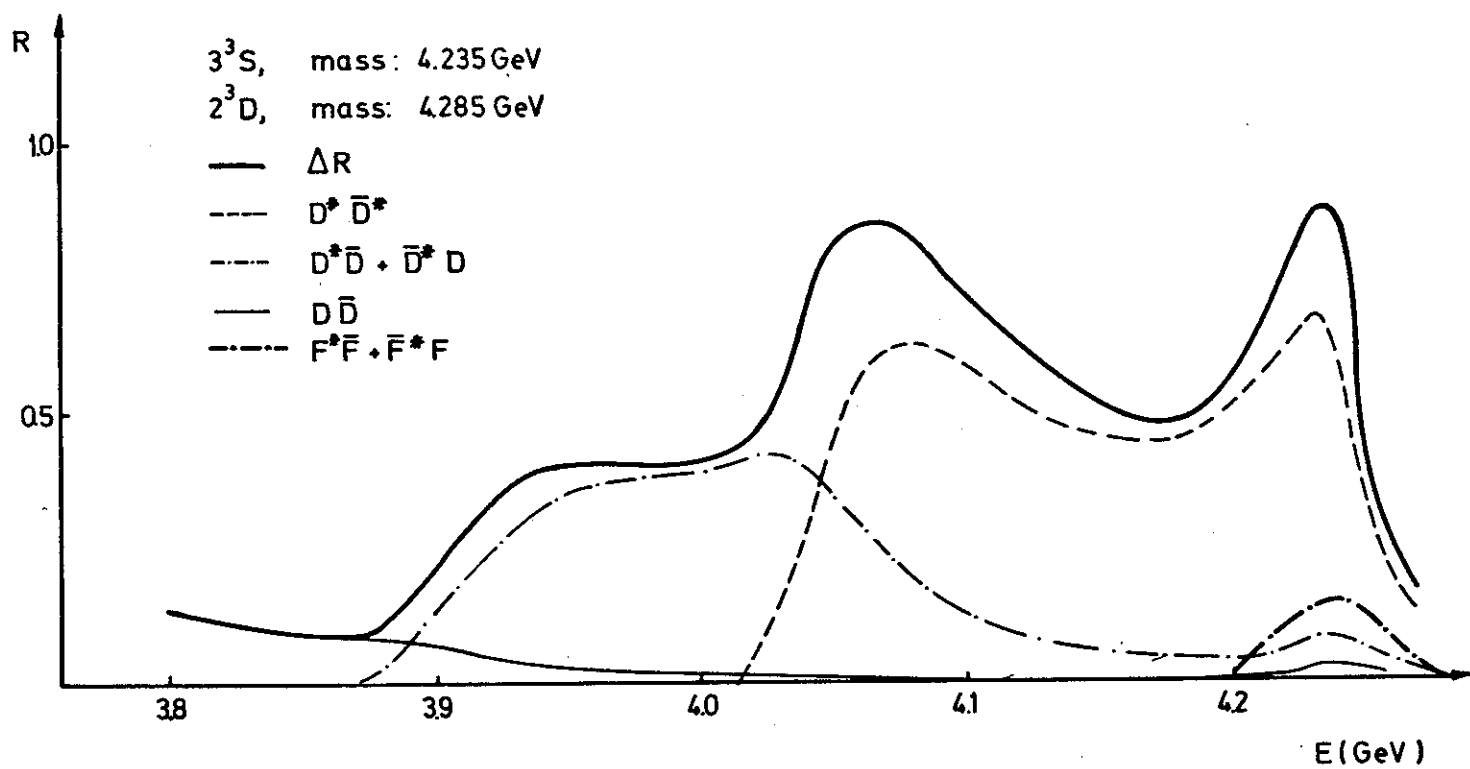


Fig. 5

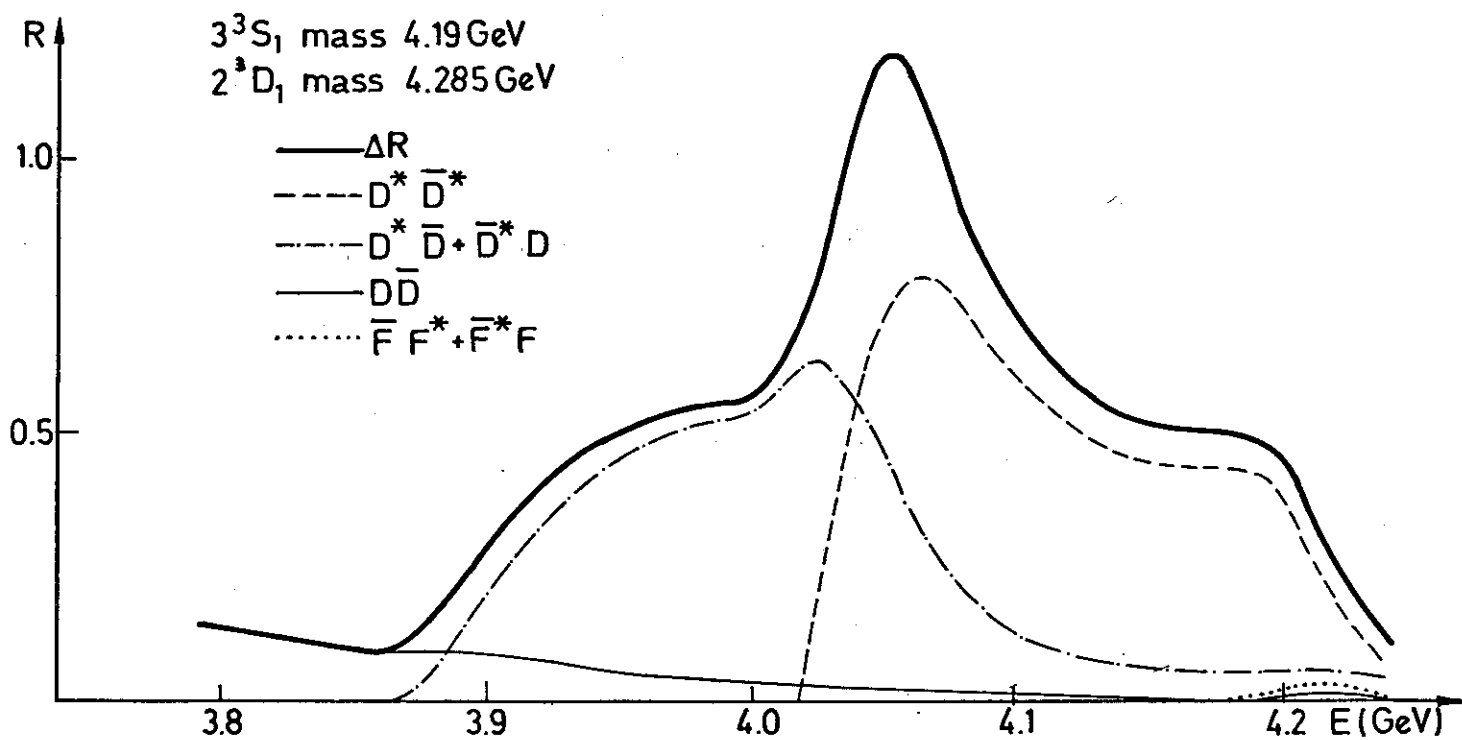


Fig.6

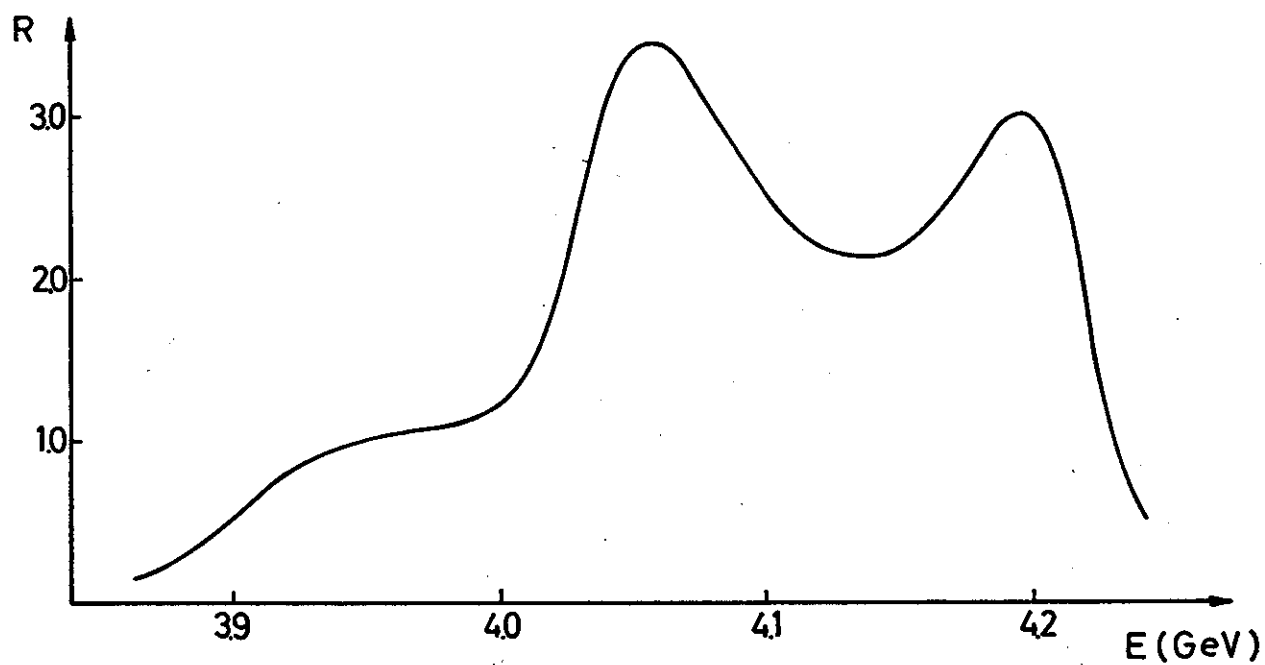


Fig.7

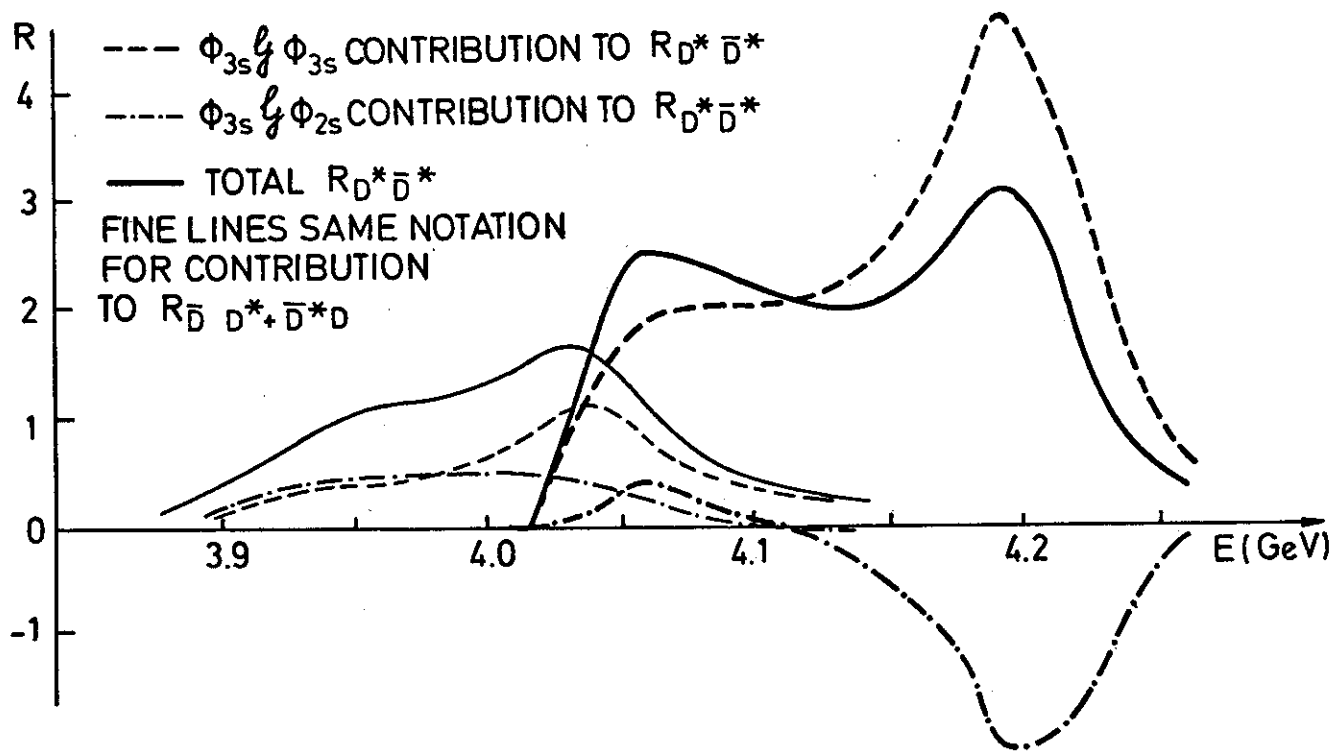


Fig. 8

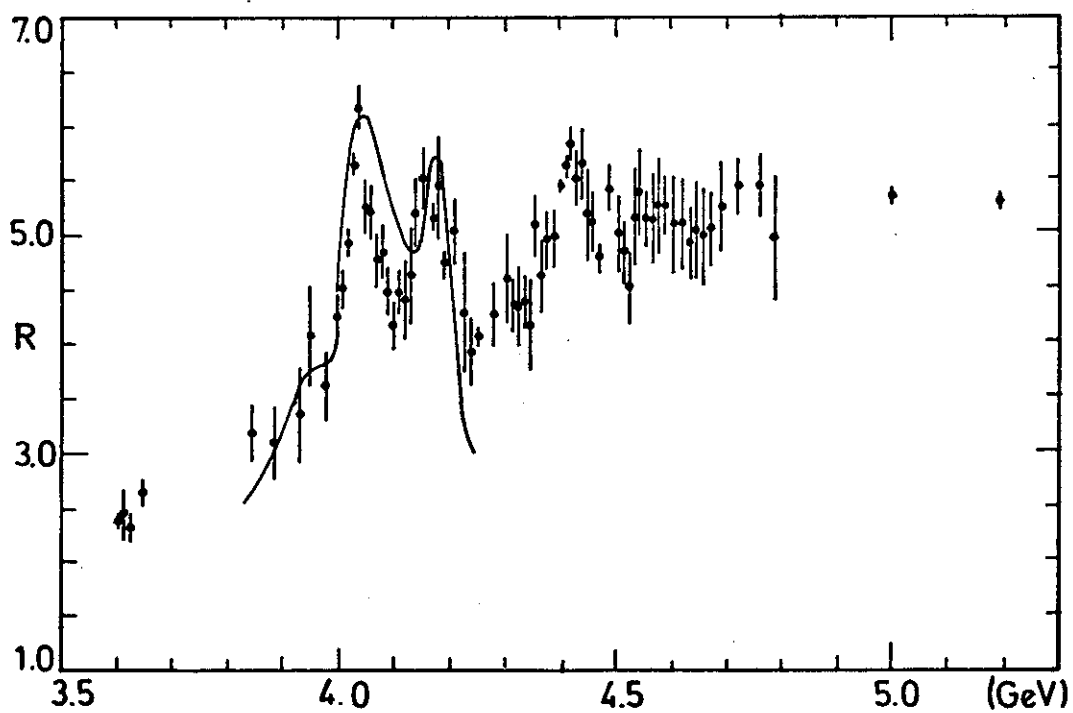


Fig. 9